

**Branching Fraction for $B^0 \rightarrow \pi^- \ell^+ \nu$ and Determination of $|V_{ub}|$
 in $\Upsilon(4S) \rightarrow B^0 \bar{B}^0$ Events Tagged by $\bar{B}^0 \rightarrow D^{(*)+} \ell^- \bar{\nu}$**

The BABAR Collaboration

November 19, 2018

Abstract

We report preliminary results from a study of the charmless exclusive semileptonic decay $B^0 \rightarrow \pi^- \ell^+ \nu$ based on the data collected at the $\Upsilon(4S)$ resonance using the BABAR detector at SLAC. The analysis uses events in which the signal B meson recoils against a B meson that has been reconstructed in a semileptonic decay $\bar{B}^0 \rightarrow D^{(*)+} \ell^- \bar{\nu}$. We extract the total branching fraction $\mathcal{B}(B^0 \rightarrow \pi^- \ell^+ \nu) = (1.03 \pm 0.25_{\text{stat.}} \pm 0.13_{\text{syst.}}) \times 10^{-4}$ and the partial branching fractions in three bins of q^2 , the invariant mass squared of the lepton-neutrino system. From the partial branching fractions and theoretical predictions for the form factors, we determine the magnitude of the CKM matrix element $|V_{ub}|$. We find $|V_{ub}| = (3.3 \pm 0.4_{\text{stat.}} \pm 0.2_{\text{syst.}}^{+0.8}_{-0.4\text{FF}}) \times 10^{-3}$, where the last error is due to normalization of the form factor.

Contributed to the XXIInd International Symposium on Lepton and Photon Interactions at High Energies, 6/30–7/5/2005, Uppsala, Sweden

Stanford Linear Accelerator Center, Stanford University, Stanford, CA 94309

Work supported in part by Department of Energy contract DE-AC03-76SF00515.

The BABAR Collaboration,

B. Aubert, R. Barate, D. Boutigny, F. Couderc, Y. Karyotakis, J. P. Lees, V. Poireau, V. Tisserand,
A. Zghiche

Laboratoire de Physique des Particules, F-74941 Annecy-le-Vieux, France

E. Grauges

IFAE, Universitat Autònoma de Barcelona, E-08193 Bellaterra, Barcelona, Spain

A. Palano, M. Pappagallo, A. Pompili

Università di Bari, Dipartimento di Fisica and INFN, I-70126 Bari, Italy

J. C. Chen, N. D. Qi, G. Rong, P. Wang, Y. S. Zhu

Institute of High Energy Physics, Beijing 100039, China

G. Eigen, I. Ofte, B. Stugu

University of Bergen, Institute of Physics, N-5007 Bergen, Norway

G. S. Abrams, M. Battaglia, A. B. Breon, D. N. Brown, J. Button-Shafer, R. N. Cahn, E. Charles,
C. T. Day, M. S. Gill, A. V. Gritsan, Y. Groysman, R. G. Jacobsen, R. W. Kadel, J. Kadyk, L. T. Kerth,
Yu. G. Kolomensky, G. Kukartsev, G. Lynch, L. M. Mir, P. J. Oddone, T. J. Orimoto, M. Pripstein,
N. A. Roe, M. T. Ronan, W. A. Wenzel

Lawrence Berkeley National Laboratory and University of California, Berkeley, California 94720, USA

M. Barrett, K. E. Ford, T. J. Harrison, A. J. Hart, C. M. Hawkes, S. E. Morgan, A. T. Watson

University of Birmingham, Birmingham, B15 2TT, United Kingdom

M. Fritsch, K. Goetzen, T. Held, H. Koch, B. Lewandowski, M. Pelizaeus, K. Peters, T. Schroeder,
M. Steinke

Ruhr Universität Bochum, Institut für Experimentalphysik 1, D-44780 Bochum, Germany

J. T. Boyd, J. P. Burke, N. Chevalier, W. N. Cottingham

University of Bristol, Bristol BS8 1TL, United Kingdom

T. Cuhadar-Donszelmann, B. G. Fulsom, C. Hearty, N. S. Knecht, T. S. Mattison, J. A. McKenna

University of British Columbia, Vancouver, British Columbia, Canada V6T 1Z1

A. Khan, P. Kyberd, M. Saleem, L. Teodorescu

Brunel University, Uxbridge, Middlesex UB8 3PH, United Kingdom

A. E. Blinov, V. E. Blinov, A. D. Bukin, V. P. Druzhinin, V. B. Golubev, E. A. Kravchenko,
A. P. Onuchin, S. I. Serebnyakov, Yu. I. Skovpen, E. P. Solodov, A. N. Yushkov

Budker Institute of Nuclear Physics, Novosibirsk 630090, Russia

D. Best, M. Bondioli, M. Bruinsma, M. Chao, S. Curry, I. Eschrich, D. Kirkby, A. J. Lankford, P. Lund,
M. Mandelkern, R. K. Mommsen, W. Roethel, D. P. Stoker

University of California at Irvine, Irvine, California 92697, USA

C. Buchanan, B. L. Hartfiel, A. J. R. Weinstein

University of California at Los Angeles, Los Angeles, California 90024, USA

S. D. Foulkes, J. W. Gary, O. Long, B. C. Shen, K. Wang, L. Zhang
University of California at Riverside, Riverside, California 92521, USA

D. del Re, H. K. Hadavand, E. J. Hill, D. B. MacFarlane, H. P. Paar, S. Rahatlou, V. Sharma
University of California at San Diego, La Jolla, California 92093, USA

J. W. Berryhill, C. Campagnari, A. Cunha, B. Dahmes, T. M. Hong, M. A. Mazur, J. D. Richman,
W. Verkerke
University of California at Santa Barbara, Santa Barbara, California 93106, USA

T. W. Beck, A. M. Eisner, C. J. Flacco, C. A. Heusch, J. Kroseberg, W. S. Lockman, G. Nesom, T. Schalk,
B. A. Schumm, A. Seiden, P. Spradlin, D. C. Williams, M. G. Wilson
University of California at Santa Cruz, Institute for Particle Physics, Santa Cruz, California 95064, USA

J. Albert, E. Chen, G. P. Dubois-Felsmann, A. Dvoretzki, D. G. Hitlin, I. Narsky, T. Piatenko,
F. C. Porter, A. Ryd, A. Samuel
California Institute of Technology, Pasadena, California 91125, USA

R. Andreassen, S. Jayatilleke, G. Mancinelli, B. T. Meadows, M. D. Sokoloff
University of Cincinnati, Cincinnati, Ohio 45221, USA

F. Blanc, P. Bloom, S. Chen, W. T. Ford, J. F. Hirschauer, A. Kreisel, U. Nauenberg, A. Olivas,
P. Rankin, W. O. Ruddick, J. G. Smith, K. A. Ulmer, S. R. Wagner, J. Zhang
University of Colorado, Boulder, Colorado 80309, USA

A. Chen, E. A. Eckhart, J. L. Harton, A. Soffer, W. H. Toki, R. J. Wilson, Q. Zeng
Colorado State University, Fort Collins, Colorado 80523, USA

D. Altenburg, E. Feltresi, A. Hauke, B. Spaan
Universität Dortmund, Institut für Physik, D-44221 Dortmund, Germany

T. Brandt, J. Brose, M. Dickopp, V. Klose, H. M. Lacker, R. Nogowski, S. Otto, A. Petzold, G. Schott,
J. Schubert, K. R. Schubert, R. Schwierz, J. E. Sundermann
Technische Universität Dresden, Institut für Kern- und Teilchenphysik, D-01062 Dresden, Germany

D. Bernard, G. R. Bonneaud, P. Grenier, S. Schrenk, Ch. Thiebaux, G. Vasileiadis, M. Verderi
Ecole Polytechnique, LLR, F-91128 Palaiseau, France

D. J. Bard, P. J. Clark, W. Gradl, F. Muheim, S. Playfer, Y. Xie
University of Edinburgh, Edinburgh EH9 3JZ, United Kingdom

M. Andreotti, V. Azzolini, D. Bettoni, C. Bozzi, R. Calabrese, G. Cibinetto, E. Luppi, M. Negrini,
L. Piemontese
Università di Ferrara, Dipartimento di Fisica and INFN, I-44100 Ferrara, Italy

F. Anulli, R. Baldini-Ferrolì, A. Calcaterra, R. de Sangro, G. Finocchiaro, P. Patteri, I. M. Peruzzi,¹
M. Piccolo, A. Zallo
Laboratori Nazionali di Frascati dell'INFN, I-00044 Frascati, Italy

¹Also with Università di Perugia, Dipartimento di Fisica, Perugia, Italy

A. Buzzo, R. Capra, R. Contri, M. Lo Vetere, M. Macri, M. R. Monge, S. Passaggio, C. Patrignani,
E. Robutti, A. Santroni, S. Tosi

Università di Genova, Dipartimento di Fisica and INFN, I-16146 Genova, Italy

G. Brandenburg, K. S. Chaisanguanthum, M. Morii, E. Won, J. Wu

Harvard University, Cambridge, Massachusetts 02138, USA

R. S. Dubitzky, U. Langenegger, J. Marks, S. Schenk, U. Uwer

Universität Heidelberg, Physikalisches Institut, Philosophenweg 12, D-69120 Heidelberg, Germany

W. Bhimji, D. A. Bowerman, P. D. Dauncey, U. Egede, R. L. Flack, J. R. Gaillard, G. W. Morton,
J. A. Nash, M. B. Nikolich, G. P. Taylor, W. P. Vazquez

Imperial College London, London, SW7 2AZ, United Kingdom

M. J. Charles, W. F. Mader, U. Mallik, A. K. Mohapatra

University of Iowa, Iowa City, Iowa 52242, USA

J. Cochran, H. B. Crawley, V. Eyges, W. T. Meyer, S. Prell, E. I. Rosenberg, A. E. Rubin, J. Yi

Iowa State University, Ames, Iowa 50011-3160, USA

N. Arnaud, M. Davier, X. Giroux, G. Grosdidier, A. Höcker, F. Le Diberder, V. Lepeltier, A. M. Lutz,
A. Oyanguren, T. C. Petersen, M. Pierini, S. Plaszczynski, S. Rodier, P. Roudeau, M. H. Schune,
A. Stocchi, G. Wormser

Laboratoire de l'Accélérateur Linéaire, F-91898 Orsay, France

C. H. Cheng, D. J. Lange, M. C. Simani, D. M. Wright

Lawrence Livermore National Laboratory, Livermore, California 94550, USA

A. J. Bevan, C. A. Chavez, I. J. Forster, J. R. Fry, E. Gabathuler, R. Gamet, K. A. George,
D. E. Hutchcroft, R. J. Parry, D. J. Payne, K. C. Schofield, C. Touramanis

University of Liverpool, Liverpool L69 7ZE, United Kingdom

C. M. Cormack, F. Di Lodovico, W. Menges, R. Sacco

Queen Mary, University of London, E1 4NS, United Kingdom

C. L. Brown, G. Cowan, H. U. Flaecher, M. G. Green, D. A. Hopkins, P. S. Jackson, T. R. McMahon,
S. Ricciardi, F. Salvatore

University of London, Royal Holloway and Bedford New College, Egham, Surrey TW20 0EX, United Kingdom

D. Brown, C. L. Davis

University of Louisville, Louisville, Kentucky 40292, USA

J. Allison, N. R. Barlow, R. J. Barlow, C. L. Edgar, M. C. Hodgkinson, M. P. Kelly, G. D. Lafferty,
M. T. Naisbit, J. C. Williams

University of Manchester, Manchester M13 9PL, United Kingdom

C. Chen, W. D. Hulsbergen, A. Jawahery, D. Kovalskyi, C. K. Lae, D. A. Roberts, G. Simi

University of Maryland, College Park, Maryland 20742, USA

G. Blaylock, C. Dallapiccola, S. S. Hertzbach, R. Kofler, V. B. Koptchev, X. Li, T. B. Moore, S. Saremi,
H. Staengle, S. Willocq

University of Massachusetts, Amherst, Massachusetts 01003, USA

R. Cowan, K. Koeneke, G. Sciolla, S. J. Sekula, M. Spitznagel, F. Taylor, R. K. Yamamoto
*Massachusetts Institute of Technology, Laboratory for Nuclear Science, Cambridge, Massachusetts 02139,
USA*

H. Kim, P. M. Patel, S. H. Robertson
McGill University, Montréal, Quebec, Canada H3A 2T8

A. Lazzaro, V. Lombardo, F. Palombo
Università di Milano, Dipartimento di Fisica and INFN, I-20133 Milano, Italy

J. M. Bauer, L. Cremaldi, V. Eschenburg, R. Godang, R. Kroeger, J. Reidy, D. A. Sanders, D. J. Summers,
H. W. Zhao

University of Mississippi, University, Mississippi 38677, USA

S. Brunet, D. Côté, P. Taras, B. Viaud
Université de Montréal, Laboratoire René J. A. Lévêque, Montréal, Quebec, Canada H3C 3J7

H. Nicholson
Mount Holyoke College, South Hadley, Massachusetts 01075, USA

N. Cavallo,² G. De Nardo, F. Fabozzi,² C. Gatto, L. Lista, D. Monorchio, P. Paolucci, D. Piccolo,
C. Sciacca

Università di Napoli Federico II, Dipartimento di Scienze Fisiche and INFN, I-80126, Napoli, Italy

M. Baak, H. Bulten, G. Raven, H. L. Snoek, L. Wilden
*NIKHEF, National Institute for Nuclear Physics and High Energy Physics, NL-1009 DB Amsterdam, The
Netherlands*

C. P. Jessop, J. M. LoSecco
University of Notre Dame, Notre Dame, Indiana 46556, USA

T. Allmendinger, G. Benelli, K. K. Gan, K. Honscheid, D. Hufnagel, P. D. Jackson, H. Kagan, R. Kass,
T. Pulliam, A. M. Rahimi, R. Ter-Antonyan, Q. K. Wong

Ohio State University, Columbus, Ohio 43210, USA

J. Brau, R. Frey, O. Igonkina, M. Lu, C. T. Potter, N. B. Sinev, D. Strom, J. Strube, E. Torrence
University of Oregon, Eugene, Oregon 97403, USA

F. Galeazzi, M. Margoni, M. Morandin, M. Posocco, M. Rotondo, F. Simonetto, R. Stroili, C. Voci
Università di Padova, Dipartimento di Fisica and INFN, I-35131 Padova, Italy

M. Benayoun, H. Briand, J. Chauveau, P. David, L. Del Buono, Ch. de la Vaissière, O. Hamon,
M. J. J. John, Ph. Leruste, J. Malclès, J. Ocariz, L. Roos, G. Therin
*Universités Paris VI et VII, Laboratoire de Physique Nucléaire et de Hautes Energies, F-75252 Paris,
France*

²Also with Università della Basilicata, Potenza, Italy

P. K. Behera, L. Gladney, Q. H. Guo, J. Panetta
University of Pennsylvania, Philadelphia, Pennsylvania 19104, USA

M. Biasini, R. Covarelli, S. Pacetti, M. Pioppi
Università di Perugia, Dipartimento di Fisica and INFN, I-06100 Perugia, Italy

C. Angelini, G. Batignani, S. Bettarini, F. Bucci, G. Calderini, M. Carpinelli, R. Cenci, F. Forti,
M. A. Giorgi, A. Lusiani, G. Marchiori, M. Morganti, N. Neri, E. Paoloni, M. Rama, G. Rizzo, J. Walsh
Università di Pisa, Dipartimento di Fisica, Scuola Normale Superiore and INFN, I-56127 Pisa, Italy

M. Haire, D. Judd, D. E. Wagoner
Prairie View A&M University, Prairie View, Texas 77446, USA

J. Biesiada, N. Danielson, P. Elmer, Y. P. Lau, C. Lu, J. Olsen, A. J. S. Smith, A. V. Telnov
Princeton University, Princeton, New Jersey 08544, USA

F. Bellini, G. Cavoto, A. D'Orazio, E. Di Marco, R. Faccini, F. Ferrarotto, F. Ferroni, M. Gaspero, L. Li
Gioi, M. A. Mazzoni, S. Morganti, G. Piredda, F. Polci, F. Safai Tehrani, C. Voena
Università di Roma La Sapienza, Dipartimento di Fisica and INFN, I-00185 Roma, Italy

H. Schröder, G. Wagner, R. Waldi
Universität Rostock, D-18051 Rostock, Germany

T. Adye, N. De Groot, B. Franek, G. P. Gopal, E. O. Olaiya, F. F. Wilson
Rutherford Appleton Laboratory, Chilton, Didcot, Oxon, OX11 0QX, United Kingdom

R. Aleksan, S. Emery, A. Gaidot, S. F. Ganzhur, P.-F. Giraud, G. Graziani, G. Hamel de Monchenault,
W. Kozanecki, M. Legendre, G. W. London, B. Mayer, G. Vasseur, Ch. Yèche, M. Zito
DSM/Dapnia, CEA/Saclay, F-91191 Gif-sur-Yvette, France

M. V. Purohit, A. W. Weidemann, J. R. Wilson, F. X. Yumiceva
University of South Carolina, Columbia, South Carolina 29208, USA

T. Abe, M. T. Allen, D. Aston, N. van Bakel, R. Bartoldus, N. Berger, A. M. Boyarski, O. L. Buchmueller,
R. Claus, J. P. Coleman, M. R. Convery, M. Cristinziani, J. C. Dingfelder, D. Dong, J. Dorfan, D. Dujmic,
W. Dunwoodie, S. Fan, R. C. Field, T. Glanzman, S. J. Gowdy, T. Hadig, V. Halyo, C. Hast, T. Hryn'ova,
W. R. Innes, M. H. Kelsey, P. Kim, M. L. Kocian, D. W. G. S. Leith, J. Libby, S. Luitz, V. Luth,
H. L. Lynch, H. Marsiske, R. Messner, D. R. Muller, C. P. O'Grady, V. E. Ozcan, A. Perazzo, M. Perl,
B. N. Ratcliff, A. Roodman, A. A. Salnikov, R. H. Schindler, J. Schwiening, A. Snyder, J. Stelzer, D. Su,
M. K. Sullivan, K. Suzuki, S. Swain, J. M. Thompson, J. Va'vra, M. Weaver, W. J. Wisniewski,
M. Wittgen, D. H. Wright, A. K. Yarritu, K. Yi, C. C. Young
Stanford Linear Accelerator Center, Stanford, California 94309, USA

P. R. Burchat, A. J. Edwards, S. A. Majewski, B. A. Petersen, C. Roat
Stanford University, Stanford, California 94305-4060, USA

M. Ahmed, S. Ahmed, M. S. Alam, J. A. Ernst, M. A. Saeed, F. R. Wappler, S. B. Zain
State University of New York, Albany, New York 12222, USA

W. Bugg, M. Krishnamurthy, S. M. Spanier
University of Tennessee, Knoxville, Tennessee 37996, USA

R. Eckmann, J. L. Ritchie, A. Satpathy, R. F. Schwitters
University of Texas at Austin, Austin, Texas 78712, USA

J. M. Izen, I. Kitayama, X. C. Lou, S. Ye
University of Texas at Dallas, Richardson, Texas 75083, USA

F. Bianchi, M. Bona, F. Gallo, D. Gamba
Università di Torino, Dipartimento di Fisica Sperimentale and INFN, I-10125 Torino, Italy

M. Bomben, L. Bosisio, C. Cartaro, F. Cossutti, G. Della Ricca, S. Dittongo, S. Grancagnolo, L. Lanceri,
L. Vitale
Università di Trieste, Dipartimento di Fisica and INFN, I-34127 Trieste, Italy

F. Martinez-Vidal
IFIC, Universitat de Valencia-CSIC, E-46071 Valencia, Spain

R. S. Panvini³
Vanderbilt University, Nashville, Tennessee 37235, USA

Sw. Banerjee, B. Bhuyan, C. M. Brown, D. Fortin, K. Hamano, R. Kowalewski, J. M. Roney, R. J. Sobie
University of Victoria, Victoria, British Columbia, Canada V8W 3P6

J. J. Back, P. F. Harrison, T. E. Latham, G. B. Mohanty
Department of Physics, University of Warwick, Coventry CV4 7AL, United Kingdom

H. R. Band, X. Chen, B. Cheng, S. Dasu, M. Datta, A. M. Eichenbaum, K. T. Flood, M. Graham,
J. J. Hollar, J. R. Johnson, P. E. Kutter, H. Li, R. Liu, B. Mellado, A. Mihalyi, Y. Pan, R. Prepost,
P. Tan, J. H. von Wimmersperg-Toeller, S. L. Wu, Z. Yu
University of Wisconsin, Madison, Wisconsin 53706, USA

H. Neal
Yale University, New Haven, Connecticut 06511, USA

³Deceased

1 INTRODUCTION

The success of the B Factories has significantly improved our knowledge of the CP violation in the quark sector. In particular, the angle β of the Unitarity Triangle has been measured to a 5% accuracy from time-dependent CP asymmetries in $b \rightarrow c\bar{c}s$ decays [1]. On the other hand, experimental determination of the other two angles and of the lengths of the two sides (with the third side normalized to unit length) have yet to achieve comparable precision. One of the two sides, the one opposite to the angle β , is of particular interest. The uncertainty of this side is dominated by the smallest element $|V_{ub}|$, which is known to about 11% precision. Improved determination of $|V_{ub}|$ therefore translates directly to a more stringent test of the Standard Model.

Charmless semileptonic decays of the B mesons provide the best probe for $|V_{ub}|$. Measurements can be done either exclusively or inclusively, i.e., with or without specifying the hadronic final state. Since both approaches suffer from significant theoretical uncertainties, it is important to pursue both types of measurements and test their consistency.

The exclusive $B \rightarrow X_u \ell \nu$ decay rates are related to $|V_{ub}|$ through form factors. In the simplest case of $B \rightarrow \pi \ell \nu$, the differential decay rate (assuming massless leptons) is given by

$$\frac{d\Gamma(B^0 \rightarrow \pi^- \ell^+ \nu)}{dq^2} = 2 \frac{d\Gamma(B^+ \rightarrow \pi^0 \ell^+ \nu)}{dq^2} = \frac{G_F^2 |V_{ub}|^2}{24\pi^3} |f_+(q^2)|^2 p_\pi^3, \quad (1)$$

where q^2 is the invariant-mass squared of the lepton-neutrino system, and p_π is the momentum of the pion in the rest frame of the B meson. The form factor (FF) $f_+(q^2)$ is calculated with a variety of theoretical models. In this paper, we consider recent calculations by Ball and Zwicky [2] based on light-cone sum rules (LCSR) and by the HPQCD [3] and FNAL [4] Collaborations based on unquenched lattice QCD (LQCD). The LCSR and LQCD calculations provide the form factor with reliable uncertainties only in limited ranges of q^2 . It is therefore necessary to extrapolate the calculated form factor using empirical functions, or to measure the partial decay rates $\Delta\Gamma(B \rightarrow \pi \ell \nu)$ with appropriate cuts on q^2 , typically chosen as $q^2 < 16 \text{ GeV}^2$ and $q^2 > 16 \text{ GeV}^2$ for use with the LCSR and LQCD calculations, respectively.

Measurements of the partial branching fractions $\Delta\mathcal{B}(B \rightarrow \pi \ell \nu)$ have been reported by CLEO [5], Belle [6], and by BABAR [7]. The CLEO and BABAR measurements reconstructed $B \rightarrow \pi \ell \nu$ events by inferring the neutrino momentum from the missing momentum; the Belle measurement used B mesons recoiling against another B meson reconstructed in semileptonic decays. BABAR has also reported a measurement of the total branching fraction $\mathcal{B}(B \rightarrow \pi \ell \nu)$ using the recoil of fully-reconstructed hadronic B decays [8].

In this paper, we report preliminary results from a study of the $B^0 \rightarrow \pi^- \ell^+ \nu$ decay, using an event sample tagged by $\bar{B}^0 \rightarrow D^{(*)+} \ell^- \bar{\nu}$ decays.⁴ A similar study of the $B^+ \rightarrow \pi^0 \ell^+ \nu$ decay is reported in a separate paper [9].

2 THE BABAR DETECTOR AND DATA SAMPLES

This measurement uses the e^+e^- colliding-beam data collected with the BABAR detector [10] at the PEP-II storage ring. Charged particles are measured by a combination of five-layer silicon microstrip tracker and a 40-layer central drift chamber, both operating in a 1.5 T magnetic field. A detector of internally reflected Cherenkov light provides charged kaon identification. A CsI(Tl)

⁴Charge-conjugate modes are implied throughout this paper.

electromagnetic calorimeter provides photon detection and, combined with the tracking detectors, electron identification. The instrumented flux return of the magnet identifies muons by their penetration through the iron absorber.

The data sample analyzed contains 232 million $e^+e^- \rightarrow B\bar{B}$ events, where $B\bar{B}$ stands for B^+B^- or $B^0\bar{B}^0$. It corresponds to an integrated luminosity of 211 fb^{-1} on the $\Upsilon(4S)$ resonance. In addition, a smaller sample (22 fb^{-1}) of off-resonance data recorded at approximately 40 MeV below the resonance is used for background subtraction and validation purposes.

We also use several samples of simulated $e^+e^- \rightarrow B\bar{B}$ events for evaluating the signal and background efficiencies. Charmless semileptonic decays $B \rightarrow X_u\ell\nu$ are simulated as a mixture of exclusive channels ($X_u = \pi, \eta, \eta', \rho,$ and ω) based on the ISGW2 model [11] and non-resonant $B \rightarrow X_u\ell\nu$ decays [12] with hadronic masses above $2m_\pi$. For the signal channels, we give weights to the simulated events in order to reproduce the q^2 distribution predicted by the recent LCSR [2] and unquenched LQCD [3, 4] calculations as well as the ISGW2 model.

3 ANALYSIS METHOD

The analysis method we use for event selection and signal yield extraction has been developed blind, i.e., without using the signal sample in the data. The procedure described in the following sections has been chosen and optimized using MC simulation to obtain the largest expected statistical significance of the partial signal yields in the three q^2 bins defined in Section 3.2.

The outline of the analysis is as follows: We look for combinations of a D^+ or D^{*+} meson and a lepton (e^- or μ^-) that are kinematically consistent with $\bar{B}^0 \rightarrow D^{(*)+}\ell^-\bar{\nu}$ decays. For each such B candidate, we define the recoil side as the tracks and calorimeter clusters that are not associated with the candidate. We search in the recoil side for a signature of a $B^0 \rightarrow \pi^-\ell^+\nu$ decay. We take advantage of the simple kinematics of the $B^0 \rightarrow \pi^-\ell^+\nu$ process to define discriminating variables, and extract the signal yield from their distributions in three bins of q^2 . Finally we calculate the total and the partial branching fractions using the signal efficiencies predicted by a Monte Carlo (MC) simulation. We correct for the data-MC efficiency differences using a control sample in which both B mesons decay to tagging modes.

3.1 Event Selection

We search for candidate $B\bar{B}$ events in which one B meson decayed as $\bar{B}^0 \rightarrow D^{(*)+}\ell^-\bar{\nu}$, where the D^{*+} meson is reconstructed in the $D^{*+} \rightarrow D^0\pi^+$ and $D^+\pi^0$ channels. The D mesons are reconstructed in the $D^0 \rightarrow K^-\pi^+, K^-\pi^+\pi^-\pi^+, K^-\pi^+\pi^0, K_S^0\pi^+\pi^-,$ and $D^+ \rightarrow K^-\pi^+\pi^+$ channels. The widths of the signal regions around the nominal D -meson masses are between $\pm 15\text{ MeV}$ and $\pm 30\text{ MeV}$, which correspond approximately to $\pm 3\sigma$ of the mass resolution. We also define sideband regions, evenly split below and above the signal regions, which are used to subtract the combinatorial background. The sideband regions are chosen to be 1.5 times wider than the signal regions. The difference between D^{*+} and D masses must be within $\pm 3\text{ MeV}$ of the nominal values.

The $D^{(*)+}$ candidates are combined with an identified electron or muon to form a $D^{(*)+}\ell^-\bar{\nu}$ candidate. The lepton must have a center-of-mass momentum⁵ $p_\ell^* > 0.8\text{ GeV}$. If the D meson was reconstructed with a charged kaon, the kaon charge and the lepton charge must have the same sign.

For each $\bar{B}^0 \rightarrow D^{(*)+}\ell^-\bar{\nu}$ candidate, we remove from the event the tracks and the neutral clusters that make up the $D^{(*)+}\ell^-\bar{\nu}$ tag. We then search for a $B^0 \rightarrow \pi^-\ell^+\nu$ candidate in the

⁵Variables denoted with a star (x^*) are measured in the $\Upsilon(4S)$ rest frame; others are in the laboratory frame

remaining part of the event. We require an identified lepton with $p_\ell^* > 0.8 \text{ GeV}$, accompanied by an oppositely charged track that is not identified as either a lepton or a kaon. To allow for the B^0 - \bar{B}^0 mixing, we do not require the two leptons in a candidate event to be oppositely charged.

The signal events we try to identify contain two neutrinos, one from each B decay. Four-momentum conservation and the invariant masses of the B mesons and neutrinos provide just the sufficient number of constraints (8) to determine the event kinematics. Referring to the $D^{(*)+}\ell^-$ system as the “ Y ” system, we first calculate the cosine of θ_{BY} , the angle between \mathbf{p}_B^* and \mathbf{p}_Y^* , as

$$\cos \theta_{BY} = \frac{2E_B^* E_Y^* - m_B^2 - m_Y^2}{2p_B^* p_Y^*}. \quad (2)$$

The energy E_B^* and momentum p_B^* of the B meson are known from the beam energies and the B^0 mass. Equation (2) assumes that a $\bar{B}^0 \rightarrow D^{(*)+}\ell^-\bar{\nu}$ decay has been correctly reconstructed, and the only undetected particle in the final state is the neutrino. If that is the case, $\cos \theta_{BY}$ should be between -1 and $+1$ within experimental resolution. If the tag has been incorrectly reconstructed, Equation (2) does not give a cosine of a physical angle, and $\cos \theta_{BY}$ is distributed more broadly.

Analogously, we can calculate the cosine of $\theta_{B\pi\ell}$, the angle between \mathbf{p}_B^* and $\mathbf{p}_{\pi\ell}^*$, as

$$\cos \theta_{B\pi\ell} = \frac{2E_B^* E_{\pi\ell}^* - m_B^2 - m_{\pi\ell}^2}{2p_B^* p_{\pi\ell}^*}. \quad (3)$$

This variable, again, should be between -1 and $+1$ for the signal events, and distributed broadly for the background.

The momenta of the two B mesons must be back-to-back in the center-of-mass frame. Given $\cos \theta_{BY}$, $\cos \theta_{B\pi\ell}$, and the directions of \mathbf{p}_Y^* and $\mathbf{p}_{\pi\ell}^*$, we can determine the direction of the B momenta up to a two-fold ambiguity. Denoting ϕ_B to be the angle between \mathbf{p}_B^* and the plane defined by \mathbf{p}_Y^* and $\mathbf{p}_{\pi\ell}^*$, we find

$$\cos^2 \phi_B = \frac{\cos^2 \theta_{BY} + \cos^2 \theta_{B\pi\ell} + 2 \cos \theta_{BY} \cos \theta_{B\pi\ell} \cos \gamma}{\sin^2 \gamma}, \quad (4)$$

where γ is the angle between \mathbf{p}_Y^* and $\mathbf{p}_{\pi\ell}^*$, as shown in Figure 1. It should be noted that $\cos^2 \phi_B$ satisfies

$$\cos^2 \phi_B \geq \cos^2 \theta_{BY} \quad \text{and} \quad \cos^2 \phi_B \geq \cos^2 \theta_{B\pi\ell} \quad (5)$$

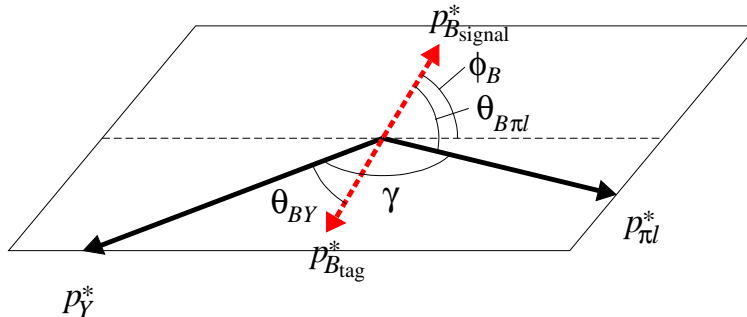


Figure 1: Angles ϕ_B , θ_{BY} , $\theta_{B\pi\ell}$, and γ . The B and \bar{B} momenta (dashed red arrows) are out of the plane defined by the Y and $\pi\ell$ momenta (black arrows).

by construction. Equation (4) assumes that $\cos\theta_{BY}$ and $\cos\theta_{B\pi\ell}$ are correct, i.e., both the tag-side and the signal-side of the event have been correctly reconstructed with only one neutrino missing on each side. In that case, the variable $\cos^2\phi_B$ must be between 0 and 1. If any part of the reconstruction is incorrect, $\cos^2\phi_B$ is no longer a cosine squared of any physical angle, and its distribution spreads beyond +1.

We use $\cos^2\phi_B$ as the principal discriminating variable for this analysis. Since $\cos^2\phi_B$ uses the information of the complete event and is strongly correlated with $\cos\theta_{BY}$ and $\cos\theta_{B\pi\ell}$, we apply only very loose cuts, $|\cos\theta_{BY}| < 5$ and $|\cos\theta_{B\pi\ell}| < 5$, in the event selection.

If a signal event has been fully reconstructed, no other particles should be present. In reality, such an event often contains extra photons, some of which come from π^0 s and/or photons from decays of D^* or heavier charmed mesons. Although we use the $D^{*+} \rightarrow D^+\pi^0$ decay in the tags, the efficiency for reconstructing the soft π^0 is low. We do not use the $D^{*+} \rightarrow D^+\gamma$ decay due to a poor signal-to-background ratio. We identify the photons that may have come from $D^* \rightarrow D\pi^0$ and $D\gamma$ decays by combining them with the D meson candidate; if the combination satisfies $m_{D\gamma} - m_D < 150$ MeV and $\cos\theta_{BY'} < 1.1$, where Y' stands for the $D\gamma\ell$ system, the photon is considered as a part of the $D^{(*)}\ell\nu$ system and is removed from the recoil system. Another source of extra photons is Bremsstrahlung in the detector material. If either lepton is an electron, we identify and remove the Bremsstrahlung photons based on their proximity to the direction of the electron track.

At this point, we require that the event contains no charged tracks besides the $\bar{B}^0 \rightarrow D^{(*)+}\ell^-\bar{\nu}$ and $B^0 \rightarrow \pi^-\ell^+\nu$ candidates. We further require that there be no residual photons with laboratory-frame energy $E_\gamma > 100$ MeV.

A few additional cuts are applied to improve the signal-to-background ratio by rejecting specific types of known background events. In order to suppress non- $B\bar{B}$ background, we require that the ratio R_2 of the second and zeroth Fox-Wolfram moments [13], computed using all charged tracks and neutral clusters in the event, be smaller than 0.5. The invariant mass of the two leptons, if they are oppositely charged, must not satisfy $2.95 < m_{e^+e^-} < 3.15$ GeV or $3.05 < m_{\mu^+\mu^-} < 3.15$ GeV in order to suppress the background due to $J/\psi \rightarrow \ell^+\ell^-$ decays. We also calculate the invariant mass of the $\pi^+\ell^-$ system assuming that the pion was a lepton of the same species as the identified lepton, and require this mass to be outside 3.06–3.12 GeV.

After all the selection cuts, a small fraction of events contain more than one candidate; simulated signal events that pass the selection contain 1.14 candidates on average. When there are multiple candidates in an event, we select the candidate with the smallest value of $|\cos\theta_{BY}|$. The candidates in the D -mass sidebands are included in the selection procedure.

3.2 Signal Yields

We find in the on-resonance data 966 ± 31 and 725 ± 34 candidate events in the D -mass signal region before and after the sideband subtraction, respectively. Table 1 summarizes the numbers of candidate events for each decay channel of $D^{(*)+}$.

We extract the signal from the $\cos^2\phi_B$ distribution in three q^2 bins, namely, $q^2 < 8$ GeV², $8 < q^2 < 16$ GeV², and $q^2 > 16$ GeV², as shown in Figure 2. For each event passing the selection, we calculate q^2 by

$$q^2 = (p_\ell + p_\nu)^2 \approx (\tilde{p}_B - p_\pi)^2, \quad (6)$$

where \tilde{p}_B is the approximate B four-momentum defined, in the center-of-mass frame, as

$$\tilde{p}_B^* = (\tilde{E}_B^*, \tilde{\mathbf{p}}_B^*) \equiv \left(\frac{m_{\Upsilon(4S)}}{2}, 0, 0, 0 \right). \quad (7)$$

Table 1: Numbers of candidate events that enter the signal-yield fit from the on-resonance data. The D -mass sidebands have been subtracted.

$D^{(*)+}$ decay channel	Events
$D^+(K^-\pi^+\pi^+)$	336.3 ± 25.2
$D^0(K^-\pi^+)\pi^+$	89.0 ± 9.9
$D^0(K^-\pi^+\pi^-\pi^+)\pi^+$	102.3 ± 11.7
$D^0(K^-\pi^+\pi^0)\pi^+$	172.7 ± 14.8
$D^0(K_S^0\pi^+\pi^-\pi^+)\pi^+$	17.7 ± 5.2
$D^+(K^-\pi^+\pi^+)\pi^0$	7.3 ± 3.4
Total	725.3 ± 33.6

In other words, the center-of-mass motion of the B meson is ignored. Since the B momentum in the center-of-mass frame is small, the impact of this approximation is small, as will be shown in Section 3.3. It is worth noting that the experimental input to Equation (6) is the pion momentum and not the lepton momentum. As a result, electron energy loss due to unrecovered Bremsstrahlung has no impact on the q^2 resolution.

The backgrounds in this measurement are handled in three groups. First, the combinatoric background for the D mesons is subtracted using the D -mass sidebands. The remaining backgrounds are mostly $B\bar{B}$ events, and are separated from the signal using the $\cos^2 \phi_B$ distribution. The possible contribution from the non- $B\bar{B}$ background is estimated, based on the $\cos^2 \phi_B$ distribution of the off-resonance data events that pass the event selection, to be smaller than 1.0 event of the total yield, and is included in the systematic error.

The raw signal yield is extracted in each q^2 bin by a simple binned χ^2 fit of the $\cos^2 \phi_B$ distribution of the on-resonance data to the weighted sum of the signal and $B\bar{B}$ background distributions from the MC simulation. The sources of the $B\bar{B}$ background can be $B \rightarrow X_u \ell \nu$ decays, $B \rightarrow X_c \ell \nu$ decays, and other (hadronic) B decays. The $\cos^2 \phi_B$ distribution for the signal events peaks between 0 and 1, while that of the background is broad with a gradual fall off toward large values of $\cos^2 \phi_B$. The fall-off is faster for smaller q^2 , as it can be seen in Figure 2. Since the $\cos^2 \phi_B$ distributions for the $B\bar{B}$ background from various sources are quite similar, we fix their relative abundances in the fit, and later vary them within their systematic uncertainties. The fit therefore has two free parameters: the normalization of the signal and the normalization of the $B\bar{B}$ background.

To maximize the statistical sensitivity, the first bin of the $\cos^2 \phi_B$ histogram should be at least as narrow as the signal peak. At the same time, each bin should contain sufficient entries to prevent the χ^2 fit from becoming biased. We use variable bin sizes to satisfy the two requirements. The bin boundaries are chosen to be $\cos^2 \phi_B = 0, 1, 2, 4, 7, \text{ and } 12$.

Table 2 summarizes the signal yield obtained from the fit of the on-resonance data, the χ^2 values (for 3 degrees of freedom) and the corresponding probabilities. The combined χ^2 probability of all three q^2 bins is 0.033. The poor χ^2 value of the last q^2 bin is caused by the large number of events in $1 < \cos^2 \phi_B < 2$. Moving the first bin boundary from 1.0 to 1.5 improves the χ^2 and increases the yield significantly. We can find no reason for this behavior other than statistical fluctuation. We therefore retain the result obtained with the original binning, which was chosen before the data were unblinded.

Table 2: Partial signal yields, χ^2 values and probabilities in bins of q^2 . The errors are statistical.

q^2 bin	Yield (events)	χ^2	Prob.
$q^2 < 8 \text{ GeV}^2$	26.3 ± 8.7	4.6	0.20
$8 < q^2 < 16 \text{ GeV}^2$	21.2 ± 9.2	1.9	0.59
$q^2 > 16 \text{ GeV}^2$	14.2 ± 8.8	11.7	0.008

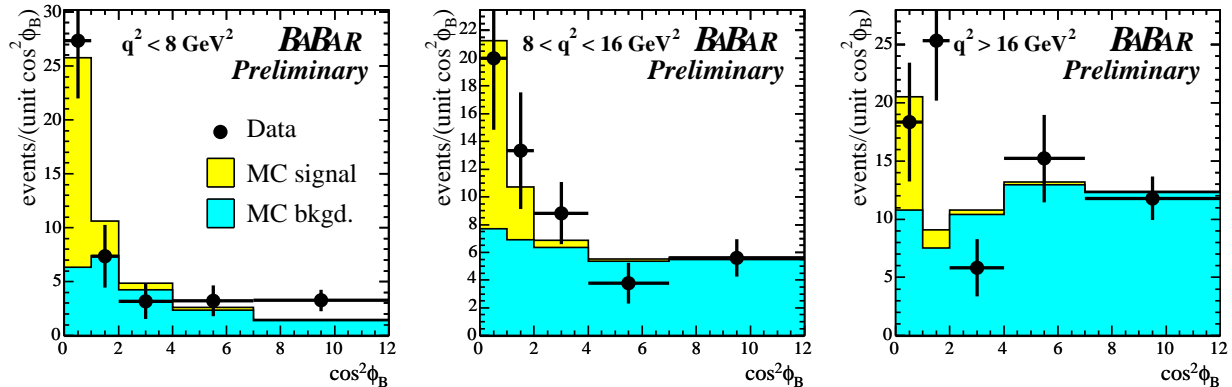


Figure 2: The $\cos^2 \phi_B$ fit of the data for $q^2 < 8 \text{ GeV}^2$ (left), $8 < q^2 < 16 \text{ GeV}^2$ (middle), and $q^2 > 16 \text{ GeV}^2$ (right). The m_D sidebands have been subtracted. The points with error bars are the on-resonance data. The histograms are signal (yellow) and $B\bar{B}$ background (cyan).

3.3 Signal Efficiencies

In order to derive the partial branching fractions from the signal yields, we need the signal efficiency in each q^2 bin. Since the measured value of q^2 from Equation (6) in principle differs from the true value, we define the efficiency ε_{ij} as the probability, averaged over electrons and muons, of a $B^0 \rightarrow \pi^- \ell^+ \nu$ event whose true q^2 value belongs to the j -th bin to be found in the i -th measured- q^2 bin. With this definition, the signal yield obtained in the i -th reconstructed- q^2 bin is expressed as

$$N_i = 2 \sum_j \varepsilon_{ij} \Delta \mathcal{B}_j N_B, \quad (8)$$

where the factor of two comes from using both electrons and muons, $\Delta \mathcal{B}_j$ is the partial branching fraction in the j -th q^2 bin, and N_B is the number of B^0 mesons in the data sample. Using the $\Upsilon(4S) \rightarrow B^0 \bar{B}^0$ branching fraction $f_{00} = 0.488 \pm 0.013$ [14], the number N_B equals $2f_{00}N_{B\bar{B}}$, where $N_{B\bar{B}}$ is the number of $B\bar{B}$ events in the data sample, and the factor of 2 comes from having two B mesons in each event.

We use the Monte Carlo simulation to estimate ε_{ij} and correct for the known data-MC differences as

$$N_i = 2 \frac{\varepsilon^{\text{data}}}{\varepsilon^{\text{MC}}} \sum_j \varepsilon_{ij}^{\text{MC}} \Delta \mathcal{B}_j N_B. \quad (9)$$

Here we assumed that a single data-MC efficiency ratio $\varepsilon^{\text{data}}/\varepsilon^{\text{MC}}$ can be applied to all q^2 bins. This is reasonable so long as the ratio is close to unity, which is in fact the case as it will be shown below.

The efficiency determined from the MC simulation is

$$\varepsilon_{ij}^{\text{MC}} = \begin{pmatrix} 1.142 \pm 0.065 & 0.050 \pm 0.011 & 0.004 \pm 0.004 \\ 0.074 \pm 0.015 & 1.232 \pm 0.071 & 0.035 \pm 0.015 \\ 0.007 \pm 0.008 & 0.063 \pm 0.016 & 1.350 \pm 0.097 \end{pmatrix} \times 10^{-3}. \quad (10)$$

The errors are due to Monte Carlo statistics. The selection efficiency averaged over the three q^2 bins is 1.32×10^{-3} . In addition to the experimental resolution, final-state radiation (FSR) changes the q^2 distribution. All MC samples used in this analysis are generated with PHOTOS [15] to simulate FSR. The bin-to-bin migration due to FSR is predicted by the MC simulation to be less than 1.2%, and the full size of this effect is included in the systematic error.

We evaluate the data-MC difference of the $\bar{B}^0 \rightarrow D^{(*)+} \ell^- \bar{\nu}$ selection efficiencies using the double-tag events, in which both B mesons decay to $D^{(*)\pm} \ell \nu$. Properties of the $D^{(*)} \ell \nu$ tags such as the composition of the $D^{(*)}$ decay channels are similar for the tagged-signal and double-tag events. The number of double-tag events is proportional to the square of the tagging efficiency after subtracting the small contribution from background.

The selection criteria for the double-tag events follow the main analysis as closely as possible. In each event, we look for two $D^{(*)} \ell \nu$ tags that do not share any particles. We remove all particles that are used in the two tags and require that there be no charged tracks and no neutral clusters remaining in the event.

After subtracting the D -mass sidebands, we find 1073.4 double-tag events in the on-resonance data. Figure 3 shows the $\cos^2 \phi_B$ distribution of the selected events. The ‘signal’ in this case consists of the $B^0 \bar{B}^0$ events in which the two B mesons decay into $D^{(*)} \ell \nu$ and are correctly reconstructed as two tags. A small fraction of $B^0 \bar{B}^0$ events with two $D^{(*)} \ell \nu$ decays are incorrectly tagged, i.e., wrong combinations of particles are selected as the two tags. Other sources of background events include $B \rightarrow \tau \rightarrow \ell$ cascade decays and lepton misidentification.

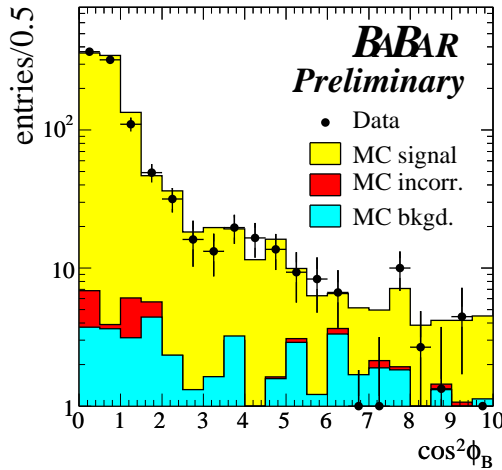


Figure 3: Distribution of $\cos^2 \phi_B$ for the double-tag events in the data (error bars) and in the MC simulation (histograms). The m_D sidebands have been subtracted. Colors indicate events with two correct tags (yellow), $B\bar{B}$ events with two $B \rightarrow D^{(*)} \ell \nu$ decays that were not correctly reconstructed (red), and other background (cyan).

We extract from the study of the double-tag events the efficiency correction factor

$$\frac{\varepsilon^{\text{data}}}{\varepsilon^{\text{MC}}} = 1.000 \pm 0.047.$$

The stated error includes both the statistical and systematic uncertainties. For the latter, we considered a) the difference in the results when the selection criteria are relaxed to allow presence of neutral clusters, b) the residual background after the D -mass sideband subtraction, due to possible non-linearities in the backgrounds vs. D mass, and c) the uncertainties in the exclusive $B \rightarrow X_c \ell \nu$ branching fractions. The relaxed criteria used in a) increase the double-tag yield and the background by approximately 50% and 100%, respectively.

4 SYSTEMATIC UNCERTAINTIES

The significant sources of systematic uncertainties and their impact on the measured total and partial branching fractions are summarized in Table 3.

For the $B \rightarrow \pi \ell \nu$ form factor, we use the Ball-Zwicky calculation for our central values, and consider the differences between that and the two LQCD calculations as the systematic uncertainties. The form factor affects the branching fractions through the q^2 dependence of the signal efficiency.

Table 3: Fractional systematic errors on the total and partial branching fractions.

Systematics	$\sigma_{\mathcal{B}}/\mathcal{B}$ (%)	$\sigma_{\Delta\mathcal{B}}/\Delta\mathcal{B}$ (%) in q^2 bins		
		$< 8 \text{ GeV}^2$	8–16 GeV^2	$> 16 \text{ GeV}^2$
$B \rightarrow \pi \ell \nu$ FF	+0.2/−0.0	+0.2/−0.7	+0.7/−0.3	+1.6/−0.3
$B \rightarrow \rho \ell \nu$ FF	+0.5/−0.0	+0.0/−0.2	+0.5/−0.0	+2.6/−0.0
$\mathcal{B}(B \rightarrow \rho \ell \nu)$	+2.9/−3.4	±0.1	±3.7	+7.8/−10.2
$\mathcal{B}(B \rightarrow X_c \ell \nu)$	±2.8	±4.8	±9.9	±13.0
$\mathcal{B}(B \rightarrow X_u \ell \nu)$	±1.7	±0.1	±1.9	±5.6
Shape Function	+0.8/−1.1	±0.1	±0.6	+2.8/−4.1
$D^{(*)} \ell \nu$ Tagging	±4.7	±4.7	±4.7	±4.7
Tracking	±1.6	±1.6	±1.6	±1.6
Electron ID	±1.1	±1.2	±1.1	±0.9
Muon ID	±1.4	±1.2	±1.4	±1.6
q^2 resolution	NA	±2.0	+0.6/−0.8	±2.9
Final-state radiation	NA	±1.2	±1.2	±1.2
$\cos^2 \phi_B$ for backgrounds	+8.8/−9.1	+5.6/−1.6	+10.1/−14.2	+14.0/−17.9
Non- $B\bar{B}$ background	±1.6	±1.6	±1.6	±1.6
Combinatoric D	±0.8	±0.8	±0.8	±0.8
$N_{B\bar{B}}$	±1.1	±1.1	±1.1	±1.1
f_{00}	±2.7	±2.7	±2.7	±2.7
MC statistics	±3.5	±5.8	±6.1	±7.6
Total	+12.2/−12.5	+11.5/−10.2	+17.2/−19.9	+24.1/−27.4

As a result, only the shape and not the normalization of the form factor is relevant at this stage, while the normalization becomes important in the determination of $|V_{ub}|$ as discussed in Section 5. The $B \rightarrow \rho\ell\nu$ decays are significant sources of background at large q^2 . We vary the branching fractions as $\mathcal{B}(B^0 \rightarrow \rho^-\ell^+\nu) = (2.69_{-0.77}^{+0.74}) \times 10^{-4}$ and $\mathcal{B}(B^+ \rightarrow \rho^0\ell^+\nu) = (1.45_{-0.41}^{+0.40}) \times 10^{-4}$, based on the measurements [16] and isospin symmetry. We also compare results using the $B \rightarrow \rho\ell\nu$ form factors calculated by Ball and Zwicky [2], Melikhov and Stech [17], and UKQCD [18].

The branching fractions for the $B \rightarrow X_c\ell\nu$ and $B \rightarrow X_u\ell\nu$ decays also significantly affect the backgrounds. We use the latest measurements [19] for the branching fractions. Where appropriate, we combine the B^0 and B^+ branching fractions assuming isospin symmetry. The shape function parameters used for the simulation of the non-resonant $B \rightarrow X_u\ell\nu$ decay are varied according to Ref. [20].

The efficiency for the $D^{(*)}\ell\nu$ tagging has been discussed in Section 3.3. The systematic uncertainties in the track reconstruction and lepton identification efficiencies have been derived from studies of independent control samples. We vary the amount of migration between the q^2 bins due to resolution, given by the off-diagonal components in Equation (10), by $\pm 50\%$. We assign an additional $\pm 1.2\%$ error on the partial branching fractions for the q^2 -bin migration due to final-state radiation, which is simulated using PHOTOS [15].

The largest source of systematic error is the shape of the $\cos^2\phi_B$ distribution for the $B\bar{B}$ background events. We studied it using several control samples that are depleted of the $\pi\ell\nu$ signal, obtained, for example, by requiring one extra charged track or neutral cluster remaining in the event. The $\cos^2\phi_B$ distributions of the control samples agree between the data and the MC simulation within the available statistics. We assign the systematic errors based on the statistical uncertainties of these tests.

We used the off-resonance data sample to set an upper limit on the residual non- $B\bar{B}$ background. MC simulation was used to determine the size of the combinatoric background that remains after the D -mass sideband subtraction, due to the non-linearities in the backgrounds vs. reconstructed D mass.

The number of $B\bar{B}$ events in the on-resonance data sample is known to $\pm 1.1\%$. We use $f_{00} = 0.488 \pm 0.013$ [14] as the $\Upsilon(4S) \rightarrow B^0\bar{B}^0$ branching fraction. Limited statistics of the MC samples affects the measurement primarily through the estimation of the signal efficiency $\varepsilon_{ij}^{\text{MC}}$ given in Equation (10).

In addition to the studies discussed above, we perform a large number of crosschecks and tests of cut-value dependences. We investigate all cases in which the variations exceed the expected statistical fluctuations, and find no indications of systematic problems.

5 RESULTS

From the signal yields and the efficiencies evaluated in Section 3, we extract the following preliminary result for the total branching fraction:

$$\mathcal{B}(B^0 \rightarrow \pi^-\ell^+\nu) = (1.03 \pm 0.25_{\text{stat.}} \pm 0.13_{\text{syst.}}) \times 10^{-4}.$$

The partial branching fractions and their statistical errors are given in Table 4. Note that the errors in the partial branching fractions are negatively correlated because of the small migration across q^2 bins, so adding them in quadrature does not give the error in the total branching fraction. We extracted the branching fractions for each of four signal form-factor calculations (Ball-Zwicky, HPQCD, FNAL, ISGW2); the differences are small.

Table 4: Preliminary results for the partial and total $B^0 \rightarrow \pi^- \ell^+ \nu$ branching fractions. The errors are statistical.

Signal FF	$\Delta\mathcal{B}(B^0 \rightarrow \pi^- \ell^+ \nu) \times 10^4$			$\mathcal{B} \times 10^4$
	$< 8 \text{ GeV}^2$	$8\text{--}16 \text{ GeV}^2$	$> 16 \text{ GeV}^2$	
Ball-Zwicky [2]	0.483 ± 0.166	0.337 ± 0.162	0.209 ± 0.140	1.029 ± 0.253
HPQCD [3]	0.480 ± 0.165	0.339 ± 0.163	0.211 ± 0.142	1.031 ± 0.254
FNAL [4]	0.483 ± 0.166	0.337 ± 0.162	0.209 ± 0.141	1.029 ± 0.253
ISGW2 [11]	0.477 ± 0.165	0.339 ± 0.163	0.215 ± 0.147	1.032 ± 0.256

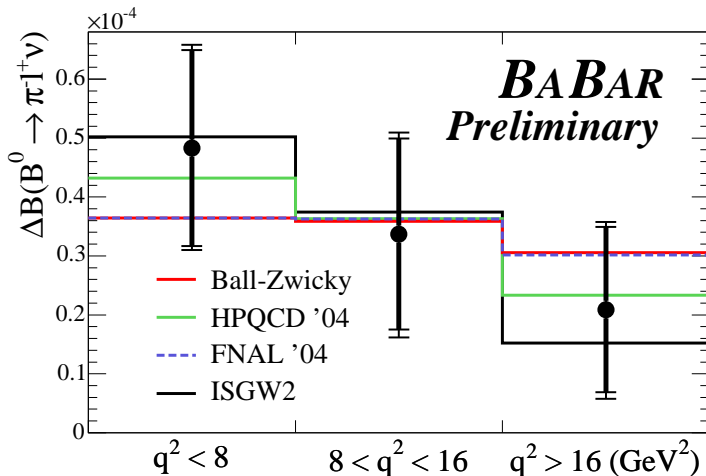


Figure 4: The partial branching fractions $\Delta\mathcal{B}(B^0 \rightarrow \pi^- \ell^+ \nu)$. The points with error bars are the measurements; the thick parts of the error bars indicate the statistical errors. The histograms are predictions by Ball-Zwicky [2] (red), HPQCD [3] (green), FNAL [4] (dashed blue), and ISGW2 [11] (black) calculations, each scaled to the measured total branching fraction. Thus only the q^2 dependences are relevant in this comparison. The Ball-Zwicky (red) and FNAL (dashed blue) lines overlap with each other.

Figure 4 compares the measured partial branching fractions with the q^2 dependence predicted by Ball-Zwicky, HPQCD, FNAL, and ISGW2 calculations. The calculations are normalized to the measured total branching fraction. Although the measured $\Delta\mathcal{B}$ values depend slightly on the form-factor calculation, the differences are too small ($< 2.5\%$) to be noticeable on this plot.

Table 5 summarizes the measurements of $\mathcal{B}(B \rightarrow \pi \ell \nu)$ by the *BABAR* collaboration. Assuming isospin symmetry and the ratio of B lifetimes $\tau_{B^+}/\tau_{B^0} = 1.081 \pm 0.015$ [19], the measurements agree with each other with $\chi^2 = 10.3$ for 5 degrees of freedom, which corresponds to a one-sided probability of 7%.

From the measurement of the partial branching fractions $\Delta\mathcal{B}$ described in this paper, we extract $|V_{ub}|$ using

$$|V_{ub}| = \sqrt{\frac{\Delta\mathcal{B}}{\Delta\zeta \cdot \tau_{B^0}}}, \quad (11)$$

Table 5: *BABAR* measurements of $\mathcal{B}(B \rightarrow \pi \ell \nu)$. All results are preliminary. The last row shows this measurement and the $B^+ \rightarrow \pi^0 \ell^+ \nu$ measurement in Ref. [9].

Technique	$\mathcal{B}(B^0 \rightarrow \pi^- \ell^+ \nu) \times 10^4$	$\mathcal{B}(B^+ \rightarrow \pi^0 \ell^+ \nu) \times 10^4$
Neutrino reco. [7]	$1.41 \pm 0.17 \pm 0.20$	$0.70 \pm 0.10 \pm 0.10$
Hadronic tag [8]	$0.89 \pm 0.34 \pm 0.12$	$0.91 \pm 0.28 \pm 0.14$
Semileptonic tag	$1.03 \pm 0.25 \pm 0.13$	$1.80 \pm 0.37 \pm 0.23$

Table 6: Preliminary results of $|V_{ub}|$ extracted from the measured partial (first three rows) and total (last three rows) branching fractions and form-factor calculations.

FF calculation	q^2 range	$\Delta\zeta$ (ps ⁻¹)	$ V_{ub} $ (10 ⁻³)
Ball-Zwicky [2]	$< 16 \text{ GeV}^2$	5.44 ± 1.43	$3.1 \pm 0.4_{\text{stat.}} \pm 0.2_{\text{syst.}}^{+0.5}_{-0.3\text{FF}}$
HPQCD [3]	$> 16 \text{ GeV}^2$	1.29 ± 0.32	$3.3 \pm 1.1_{\text{stat.}} \pm 0.5_{\text{syst.}}^{+0.5}_{-0.3\text{FF}}$
FNAL [4]	$> 16 \text{ GeV}^2$	1.83 ± 0.50	$2.7 \pm 0.9_{\text{stat.}} \pm 0.4_{\text{syst.}}^{+0.5}_{-0.3\text{FF}}$
Ball-Zwicky [2]	full	7.74 ± 2.32	$2.9 \pm 0.4_{\text{stat.}} \pm 0.2_{\text{syst.}}^{+0.6}_{-0.4\text{FF}}$
HPQCD [3]	full	5.70 ± 1.71	$3.4 \pm 0.4_{\text{stat.}} \pm 0.2_{\text{syst.}}^{+0.7}_{-0.4\text{FF}}$
FNAL [4]	full	6.24 ± 2.12	$3.3 \pm 0.4_{\text{stat.}} \pm 0.2_{\text{syst.}}^{+0.8}_{-0.4\text{FF}}$

where $\tau_{B^0} = 1.536 \pm 0.014 \text{ ps}$ [19] is the B^0 lifetime, and $\Delta\zeta$ is defined as

$$\Delta\zeta = \frac{G_F^2}{24\pi^3} \int_{q_{\text{min}}^2}^{q_{\text{max}}^2} |f_+(q^2)|^2 p_\pi^3 dq^2. \quad (12)$$

To minimize the theoretical error on $|V_{ub}|$, the range of q^2 should correspond to the region in which the form-factor calculation is most reliable: $q^2 < 16 \text{ GeV}^2$ for LCSR and $q^2 > 16 \text{ GeV}^2$ for LQCD. In order to extract $|V_{ub}|$ from the total branching fraction \mathcal{B} , the form factor must be extrapolated to the full range of q^2 . This is done in Refs. [2, 3, 4] using empirical functions, and additional uncertainties are assigned for the extrapolation.

Table 6 summarizes the values of $|V_{ub}|$ extracted from the measured partial and total branching fractions. The last errors on $|V_{ub}|$ come from the uncertainties in $\Delta\zeta$, which in turn come from the uncertainties of the normalization of the form-factor calculations. The precision of the results obtained using the LQCD calculations [3, 4] in $q^2 > 16 \text{ GeV}^2$ are limited by the large statistical error of the measured partial branching fraction. Using the total branching fraction reduces experimental errors on $|V_{ub}|$ at the cost of increased theoretical uncertainties due to the extrapolation of the form factor.

Instead of averaging results based on different theoretical calculations, we report the value of $|V_{ub}|$ obtained from the total branching fraction based on one of the LQCD calculations [4],

$$|V_{ub}| = (3.3 \pm 0.4_{\text{stat.}} \pm 0.2_{\text{syst.}}^{+0.8}_{-0.4\text{FF}}) \times 10^{-3}.$$

as a representative result. This result lies between the results based on the other two calculations, and carries the most conservative theoretical uncertainty.

6 SUMMARY

Using event samples tagged by $\bar{B}^0 \rightarrow D^{(*)+} \ell^- \bar{\nu}$ decays, we obtain the exclusive branching fraction $\mathcal{B}(B^0 \rightarrow \pi^- \ell^+ \nu)$. The preliminary result for the total branching fraction is

$$\mathcal{B}(B^0 \rightarrow \pi^- \ell^+ \nu) = (1.03 \pm 0.25_{\text{stat.}} \pm 0.13_{\text{syst.}}) \times 10^{-4}.$$

We also obtain the partial branching fractions in three bins of q^2 of the lepton-neutrino pair. The preliminary results are

$$\Delta\mathcal{B}(B^0 \rightarrow \pi^- \ell^+ \nu) = \begin{cases} (0.48 \pm 0.17_{\text{stat.}}^{+0.06}_{-0.05\text{syst.}}) \times 10^{-4} & q^2 < 8 \text{ GeV}^2, \\ (0.34 \pm 0.16_{\text{stat.}}^{+0.06}_{-0.07\text{syst.}}) \times 10^{-4} & 8 < q^2 < 16 \text{ GeV}^2, \\ (0.21 \pm 0.14_{\text{stat.}}^{+0.05}_{-0.06\text{syst.}}) \times 10^{-4} & q^2 > 16 \text{ GeV}^2. \end{cases}$$

Using the measured total branching fraction and a form-factor calculation based on lattice QCD [4], we extract

$$|V_{ub}| = (3.3 \pm 0.4_{\text{stat.}} \pm 0.2_{\text{syst.}}^{+0.8}_{-0.4\text{FF}}) \times 10^{-3}.$$

where the last error is due to normalization of the form-factor. We also use other recent calculations of the form factor [2, 3] and find values of $|V_{ub}|$, given in Table 6, that are consistent within the experimental and theoretical uncertainties.

7 ACKNOWLEDGMENTS

We are grateful for the extraordinary contributions of our PEP-II colleagues in achieving the excellent luminosity and machine conditions that have made this work possible. The success of this project also relies critically on the expertise and dedication of the computing organizations that support *BABAR*. The collaborating institutions wish to thank SLAC for its support and the kind hospitality extended to them. This work is supported by the US Department of Energy and National Science Foundation, the Natural Sciences and Engineering Research Council (Canada), Institute of High Energy Physics (China), the Commissariat à l’Energie Atomique and Institut National de Physique Nucléaire et de Physique des Particules (France), the Bundesministerium für Bildung und Forschung and Deutsche Forschungsgemeinschaft (Germany), the Istituto Nazionale di Fisica Nucleare (Italy), the Foundation for Fundamental Research on Matter (The Netherlands), the Research Council of Norway, the Ministry of Science and Technology of the Russian Federation, and the Particle Physics and Astronomy Research Council (United Kingdom). Individuals have received support from CONACyT (Mexico), the A. P. Sloan Foundation, the Research Corporation, and the Alexander von Humboldt Foundation.

References

- [1] *BABAR* Collaboration, B. Aubert *et al.*, Phys. Rev. Lett. **94**, 161803 (2005);
Belle Collaboration, K. Abe *et al.*, Phys. Rev. D **71**, 072003 (2005), Erratum-ibid. D **71**, 079903 (2005).
- [2] P. Ball and R. Zwicky, Phys. Rev. D **71**, 014015 (2005);
P. Ball and R. Zwicky, Phys. Rev. D **71**, 014029 (2005).

- [3] J. Shigemitsu *et al.*, *Semileptonic B decays with $N_f = 2+1$ dynamical quarks*, hep-lat/0408019, Contribution to Lattice 2004, Batavia, June 21–26, 2004.
- [4] M. Okamoto *et al.*, *Semileptonic $D \rightarrow \pi/K$ and $B \rightarrow \pi/D$ decays in $2+1$ flavor lattice QCD*, hep-lat/0409116, Contribution to Lattice 2004, Batavia, June 21–26, 2004.
- [5] CLEO Collaboration, S. B. Athar *et al.*, Phys. Rev. D **68**, 072003 (2003).
- [6] Belle Collaboration, K. Abe *et al.*, *Measurement of exclusive $B \rightarrow X_u \ell \nu$ decays with $D^{(*)} \ell \nu$ decay tagging*, hep-ex/0408145, Contribution to ICHEP 2004, Beijing, August 16–22, 2004.
- [7] BABAR Collaboration, B. Aubert *et al.*, *Study of $B \rightarrow \pi \ell \nu$ and $B \rightarrow \rho \ell \nu$ decays and determination of $|V_{ub}|$* , hep-ex/0507003, Submitted to Phys. Rev. D (Rapid Comm.)
- [8] BABAR Collaboration, B. Aubert *et al.*, *Study of $b \rightarrow u \ell \bar{\nu}$ decays on the recoil of fully reconstructed B mesons and determination of $|V_{ub}|$* , hep-ex/0408068, Contribution to ICHEP 2004, Beijing, August 16–22, 2004.
- [9] BABAR Collaboration, B. Aubert *et al.*, *Branching fraction for $B^+ \rightarrow \pi^0 \ell^+ \nu$, measured in $\Upsilon(4S) \rightarrow B \bar{B}$ events tagged by $B^- \rightarrow D^0 \ell^- \bar{\nu}(X)$ decays*, hep-ex/0506065, Contribution to Lepton-Photon 2005, Uppsala, June 30–July 5, 2005.
- [10] BABAR Collaboration, B. Aubert *et al.*, Nucl. Instrum. Meth. A **479**, 1–116 (2002).
- [11] D. Scora and N. Isgur, Phys. Rev. D **52**, 2783 (1995).
- [12] F. De Fazio and M. Neubert, JHEP 9906, 017 (1999).
- [13] G. C. Fox and S. Wolfram, Phys. Rev. Lett. **41**, 1581 (1978).
- [14] CLEO Collaboration, J. P. Alexander *et al.*, Phys. Rev. Lett. **86**, 2737 (2001);
BABAR Collaboration, B. Aubert *et al.*, Phys. Rev. D **65**, 032001 (2002);
CLEO Collaboration, S. B. Athar *et al.*, Phys. Rev. D **66**, 052003 (2002).
- [15] E. Barberio and Z. Was, Comp. Phys. Commun. **79**, 291 (1994).
- [16] CLEO Collaboration, S. B. Athar *et al.*, Phys. Rev. D **68**, 072003 (2003);
BABAR Collaboration, B. Aubert *et al.*, Phys. Rev. Lett. **90**, 181801 (2003).
- [17] D. Melikhov and B. Stech, Phys. Rev. D **62**, 014006 (2000).
- [18] UKQCD Collaboration, L. Del Debbio *et al.*, Phys. Lett. B **416**, 392 (1998).
- [19] Particle Data Group, S. Eidelman *et al.*, Phys. Lett. B **592**, 1 (2004).
- [20] A. Limosani and T. Nozaki (of the Belle Collaboration for the Heavy Flavor Averaging Group), *Extraction of the b-quark shape function parameters using the Belle $B \rightarrow X_s \gamma$ photon energy spectrum*, hep-ex/0407052.